Modeling reactive geochemical transport of concentrated aqueous solutions

Guoxiang Zhang, Zuoping Zheng, and Jiamin Wan

Earth Science Division, Lawrence Berkeley National Laboratory, University of California, Berkeley, California, USA

Received 11 February 2004; revised 13 October 2004; accepted 7 December 2004; published 17 February 2005.

[1] Aqueous solutions with ionic strength larger than 1 M are usually considered concentrated aqueous solutions. These solutions can be found in some natural systems and are also industrially produced and released into accessible natural environments, and as such, they pose a big environmental problem. Concentrated aqueous solutions have unique thermodynamic and physical properties. They are usually strongly acidic or strongly alkaline, with the ionic strength possibly reaching 30 M or higher. Chemical components in such solutions are incompletely dissociated. The thermodynamic activities of both ionic and molecular species in these solutions are determined by the ionic interactions. In geological media the problem is further complicated by the interactions between the solutions and sediments and rocks. The chemical composition of concentrated aqueous solutions when migrating through the geological media may be drastically altered by these strong fluid-rock interactions. To effectively model reactive transport of concentrated aqueous solutions, we must take into account the ionic interactions. For this purpose we substantially extended an existing reactive transport code, BIO-CORE$^{2D©}$, by incorporating a Pitzer ion interaction model to calculate the ionic activity. In the present paper, the model and two test cases of the model are briefly introduced. We also simulate a laboratory column experiment in which the leakage of highly alkaline waste fluid stored at Hanford (a U.S. Department of Energy site, located in Washington State) was studied. Our simulation captures the measured pH evolution and indicates that all the reactions controlling the pH evolution, including cation exchanges and mineral dissolution/precipitation, are coupled.

Citation: Zhang, G., Z. Zheng, and J. Wan (2005), Modeling reactive geochemical transport of concentrated aqueous solutions, *Water Resour. Res.*, *41*, W02018, doi:10.1029/2004WR003097.

1. Introduction

[2] Concentrated aqueous solutions are in general defined as aqueous solutions with ionic strength larger than 1 M. Such solutions occur in many natural and contaminated environments, including seawater evaporation and intrusion [*Harvie and Weare*, 1980; *Harvie et al.*, 1984; *Krumgalz*, 2001], industrial kraft pulp mills and bayer processes [*Gerson and Zheng*, 1997; *Park and Englezos*, 1999], toxic waste solutions [*van Gaans and Schuiling*, 1997; *Gephart and Lundgren*, 1998], leakage of electrolytic fluids from storage tanks, and acid mine drainage [*Blowes et al.*, 1991]. Concentrated aqueous solutions are significantly different from dilute solutions in transport and geochemical processes because of their large density, viscosity, and complicated ionic interactions. Thus numerically modeling these solutions remains a challenge, because most geochemical reactive transport models are based on ideal (dilute) aqueous solutions, which are not applicable to concentrated aqueous solutions [*Pitzer*, 1991; *Oldenburg and Pruess*, 1995]. For instance, a significant amount of highly concentrated (up to more than 10 M) radioactive waste fluids have leaked from some of the 149 single-shell and 28 double-shell underground tanks at the U.S. Department of Energy's (DOE) Hanford site (Richland, Washington), and the local groundwater system has been contaminated. For study of fluid migration and the contamination of the groundwater system, a special numerical modeling effort that captures the effects of ionic interactions of concentrated aqueous solutions is required.

[3] Pitzer's ion interaction theory [*Pitzer*, 1973] is often used to study ionic activity in concentrated aqueous solutions. *Harvie and Weare* [1980] and *Harvie et al.* [1984] developed an ion interaction equilibrium model (HMW model) for the seawater system (Na-K-Mg-Ca-Cl-SO_4-H_2O) based on the Pitzer's ion interaction theoretical model. The HMW model was implemented in several computer codes: PHRQPITZ [*Plummer et al.*, 1988], EQ3/6 [*Wolery and Daveler*, 1992], GMIN [*Felmy*, 1995], and UNSATCHEM-2D [*Simunek and Suarez*, 1994]. On the basis of work by *Harvie and Weare* [1980], *Plummer et al.* [1988] included in their model Fe(II), Mn, Ba, Sr, Li, and Br under higher temperature (60°C) and pressure enabling calculations useful for hydrothermal systems. GMIN and UNSATCHEM-2D also provide an extension to the HMW model by including borate components. Recently, on the basis of previous studies, *Risacher and Clement* [2001] presented a pure chemical equilibrium model (EQL/EVP) for simulating evaporation of natural waters at high concentrations.

0043-1397/05/2004WR003097$09.00

[4] To estimate tank supernate compositions from historical tank inventory data at Hanford, *Lichtner and Felmy* [2003] performed simulations based on a combination of the computer code GMIN [*Felmy*, 1995] and the reactive transport code FLOTRAN [*Lichtner*, 2001]. *Steefel et al.* [2003] simulated the multiple cation exchanges taking place in the sediments of Hanford under highly alkaline conditions. Their simulation confirmed that multisite cation exchange is a very important process in controlling cesium migration in Hanford site sediment. *Lichtner et al.* [2004] also simulated the cesium migration in the context of competitive cation exchange in the vadose zone of the same site, using FLOTRAN incorporating GMIN. These authors calibrated their model using the field-measured concentrations of Na^+, NO_3^-, Ca^{2+}, and pH.

[5] High concentrations lead to a strong influence on fluid physical properties such as density and viscosity. Moreover, within geological media, flow and transport of the concentrated solutions may be affected by the density and viscosity changes induced by concentration and chemical composition changes. Several abbreviated formulations for density and viscosity changes have been used in numerical models to simulate the transport of concentrated aqueous solutions [*Voss and Souza*, 1987; *Herbert et al.*, 1988; *Oldenburg and Pruess*, 1995; *Boufadel et al.*, 1999]. However, most of these models consider only simple chemistry and neglect ionic interactions. In fact, the density of the concentrated aqueous solutions is determined by the ionic interactions and can be formulated using Pitzer-type equations, as done by *Monnin* [1994]. In this model, the density of concentrated aqueous solutions is formulated as a function of the concentrations of the chemical components, using Pitzer-type equations. Using this model, the simulated densities of the concentrated aqueous solutions of various salts match measurements well. So far, however, there is no reported model that has used the Pitzer-type equations for calculating the density changes in reactive transport simulations.

[6] The present work was motivated by a modeling study regarding the leakages of the highly alkaline-saline waste-tank solutions at the Hanford site. In this paper, we present (1) mathematical equations of the Pitzer ion interaction model for calculating activity, (2) the implementation of the Pitzer ion interaction model into the existing biogeochemical computer code, BIO-CORE^{2D} [*Zhang*, 2001], (3) the development of a database for temperature-dependent Pitzer ion interaction parameters, (4) two test cases comparing our numerical results with the reported experimental data of activity coefficients, and finally, (5) the applications of our Pitzer ion interaction model to a laboratory experiment extracted from the Hanford site, from which pH measurements were available for comparison. The application involves unsaturated flow, cation exchanges, and mineral dissolution/precipitation.

[7] The Pitzer-type density model presented by *Monnin* [1994] was also implemented in the developed code and validated using our laboratory measurements. This work will be reported in a later paper, because of the space limitations on the present paper.

2. Pitzer's Ionic Activity Model

[8] In a given aqueous solution, the thermodynamic activity of a dissolved species is calculated as the product of its concentration and its activity coefficient. The coefficient of each species is related to a corresponding partial derivative of the excess Gibbs energy of the solution, and can be formulated as a function of the concentrations and properties of the solutes in the solution [*Pitzer*, 1991]. It is also dependent on temperature, not only through the temperature dependency of each individual chemical species' thermodynamic properties in the solution, but also through the temperature-dependent ionic interactions.

[9] For dilute solutions (ionic strength smaller than 1 M), values of the activity coefficient are commonly calculated according to the Debye-Hückel formula (Appendix A) and its variations [*Wolery and Daveler*, 1992]. These formulas are expressed as a function of the ionic strength rather than any individual ionic molalities and thermodynamic properties of other species. The excess solution free energy subjected to the ionic interactions of specific ionic pairs is not considered in the formula. However, the excess solution free energy becomes significant in highly concentrated solutions, and hence the Debye-Hückel formula (including its variations) is not suitable for calculations of ionic activity in concentrated aqueous solutions [*Bethke*, 1996; *Pitzer*, 1973; *Wolery and Daveler*, 1992]. A quantitative description of the effects of ionic interactions on ionic activity in concentrated aqueous solutions requires a self-consistent model capable of evaluating ionic activity coefficients as a function of ionic strength, composition (concentrations), temperature, and pressure. The Pitzer ion interaction model [*Pitzer*, 1973] can accurately quantify the activity coefficients as well as the other thermodynamic properties of the concentrated aqueous solutions, as a function of the variables mentioned above. This semiempirical model consists of several virial equations, sometimes called specific interaction equations, Pitzer equations or phenomenological equations. These equations can adequately express the thermodynamic properties of the concentrated solution over a wide range of concentrations and temperatures [*Clegg and Whitfield*, 1991].

[10] The Pitzer model, based on a virial expansion [*Pitzer*, 1973, 1991], is reduced to a modified form of the Debye-Hückel formula at low ionic strength [*Pitzer*, 1991]. This virial expansion involves summations over all possible binary and ternary short-range interaction terms as well as mixing terms. A generally accepted form of the Pitzer model is formulated by *Harvie et al.* [1984] and called the HMW model. This model has been implemented in several computer codes such as PHRQPITZ [*Plummer et al.*, 1988], EQ3/6 [*Wolery and Daveler*, 1992], GMIN [*Felmy*, 1995] and UNSATCHEM-2D [*Simunek and Suarez*, 1994]. However, pressure dependence is not accounted for in this model.

[11] In the HMW model, water activity, a_{H_2O}, osmotic coefficient, ϕ, activity coefficients of cations, γ_M, anions, γ_X, and neutral species, γ_N, are mathematically expressed as the following equations:

$$Ln\ a_{H_2O} = -\frac{W}{1000}\left(\sum_{i=1}^{N_T} m_i\right)\phi \tag{1}$$

$$\sum_{i=1}^{N_T} m_i(\phi - 1) = 2\left[\left(-\frac{A^{\Phi} I_2^3}{1 + 1.2\sqrt{I}}\right) + \sum_{c=1}^{N_c}\sum_{a=1}^{N_a} m_c m_a \left(B_{ca}^{\Phi} + ZC_{ca}\right) + \sum_{n=1}^{N_n}\sum_{c=1}^{N_c} m_n m_c \lambda_{nc} + \sum_{n=1}^{N_n}\sum_{a=1}^{N_a} m_n m_a \lambda_{na}\right] \tag{2}$$

$$\ln \gamma_M = Z_M^2 F + \sum_{a=1}^{N_a} m_a (2B_{Ma} + ZC_{Ma}) + |Z_M| \sum_{c=1}^{N_c} \sum_{a=1}^{N_a} m_c m_a C_{ca} + 2 \sum_{n=1}^{N_n} m_n \lambda_{nM} \quad (3)$$

$$\ln \gamma_X = Z_X^2 F + \sum_{c=1}^{N_c} m_c (2B_{cX} + ZC_{cX}) + |Z_x| \sum_{c=1}^{N_c} \sum_{a=1}^{N_a} m_c m_a C_{ca} + 2 \sum_{n=1}^{N_n} m_n \lambda_{nX} \quad (4)$$

$$\ln \gamma_N = \sum_{a=1}^{N_a} m_a (2\lambda_{Na}) + \sum_{c=1}^{N_c} m_c (2\lambda_{Nc}) \quad (5)$$

where m_i, m_c, and m_a, are the molality of species i, c, and a, respectively; W is the molecular weight of water; N_T is the number of species in the system; I is solution ionic strength; subscripts M and c denote cations; X and a denote anions; N and n denote neutral species; and i denotes all species in the solution. As implied in the equations, the capital letters M, X, and N denote subject species (e.g., the species for which the activity coefficient is calculated), while c, a, and n denote, respectively, the cations, anions, and neutral species interacting with the subject ions or with each others. N_c, N_a, and N_n are the numbers of the cations, anions, and neutral species, respectively, interacting with the subject ions, and normally are the total numbers of the cations, anions, and neutral species in the system. Z_M and Z_X are the electrical charges of the subject cation M and the subject anion X, respectively; λ_{na}, λ_{Na}, and λ_{nX} are coefficients of the interactions between the neutral species and the anions, and λ_{nc}, λ_{Nc} and, λ_{nM} are the coefficients of the interactions between the neutral species and the cations. F is the modified Debye-Hückel term, Z is the solution electrical charge, A^{Φ} is one third of the Debye-Hückel limiting slope. B^{Φ}_{ca}, B_{MX} (representing B_{Ma} and B_{cX}), B'_{MX} (representing B'_{Ma} and B'_{cX}), α_{MX}, and C_{MX} (representing C_{Ma}, C_{cX} and C_{ca}) are Pitzer virial coefficients. All of these variables are given in Appendix B.

[12] The mean ionic activity coefficient, $\gamma_{\pm}$, is commonly used for calculating solute activity coefficients in concentrated aqueous solutions and is defined as:

$$Ln\,\gamma_{\pm} = (\nu_M \ln \gamma_M + \nu_X \ln \gamma_X)/\nu \quad (6)$$

where ν_M and ν_X are the stoichiometric coefficients of cations and anions in the compound formula, respectively, and $\nu = \nu_M + \nu_X$.

[13] Note that the binary interactions between ions of like signs, and the ternary interactions (e.g., interactions among one ion and two dissimilar ions of opposite signs, also regarded as mixing terms), are not considered in the present model, because the mixing terms make relatively much smaller contributions to the activity coefficients than the contributions from the interactions of binary ionic pairs with opposite signs [*Pitzer and Kim*, 1974]. By neglecting the mixing terms and the interaction terms of the like sign pairs, computational time is significantly saved – a vital advantage for reactive transport simulations. As shown in the model test cases (section 5), this simplification does not significantly affect the simulated results for solutions with ionic strength lower than 7 M. However, the contributions from the omitted terms for solutions with higher (than 7 M) ionic strength are larger, and the effects of this omission for these solutions need to be evaluated with additional tests against experimental data. This evaluation is beyond the scope of this paper.

[14] The total volume of a concentrated aqueous solution is made up of the water volume, the partial volume of the solutes, and the excess volume induced by the ionic interactions. For solutions with ionic strength larger than 0.1 M, the partial volume of solutes and the excess volume become significant. The apparent water density in concentrated aqueous solutions varies depending on the concentrations [*Dougherty*, 2001], owing to the ion-water molecule interaction. However, this variation has not been well formulated for complicated solutions and is considered to be a minor contribution to the solution density [*Monnin*, 1994], compared to the contributions from solute partial volume and the excess volume. The partial volume of solutes is a linear function of concentration and can be calculated, and this calculation must obey the ionic volume conservation law. The excess volume is relevant to the solution free energy change and can also be formulated as a function of concentrations using the Pitzer virial equations [*Pitzer*, 1991; *Monnin*, 1994]. Accounting for these three contributions, the density of concentrated aqueous solutions in the present model is calculated using the formulation and the virial parameters given by *Monnin* [1994]. Nine major ions (Na^+, K^+, Ca^{+2}, Mg^{+2}, Cl^-, SO_4^{-2}, HCO_3^-, NO_3^- and CO_3^{-2}) have been considered to significantly contribute to the solution density. Other ions are easy to add into the model if their virial coefficients are known or they can be calibrated by inverting the model.

3. Numerical Implementation

[15] The Pitzer ion interaction (HMW) model was implemented, for the work presented in this paper, into an existing reactive biogeochemical transport computer code, BIO-CORE^{2D} [*Zhang*, 2001]. This code was developed at the University of La Coruña, Spain, based on TRANQUE [*Xu et al.*, 1999] and CORE^{2D} [*Samper et al.*, 2000]. The Debye-Hückel formula was originally used in the code. Thus activity coefficients can be calculated using either the Pitzer model or Debye-Hückel model, according to user option, or an automatic switch between the two models, according to a prescribed threshold of ionic strength. The Pitzer model is used for ionic strength greater than 1 M, while the Debye-Hückel model is used for saving computation time when dealing with dilute solutions. BIO-CORE^{2D} solves the nonlinear algebraic equation system of the chemical system using the Newton-Raphson iteration method, which requires calculating the derivatives of the ionic activity with respect to the concentrations of primary species. These derivatives are analytically derived from equations (1) through (5) and implemented into the program.

[16] BIO-CORE^{2D} describes the hydrogeochemical system as an integration of migration and transformation of substance and energy in the subsurface. The simulator can accommodate any number of chemical species, including aqueous and adsorbed species and minerals, and any number of microbiological species, in both attached phase and dissolved species (in water). A wide range of subsurface

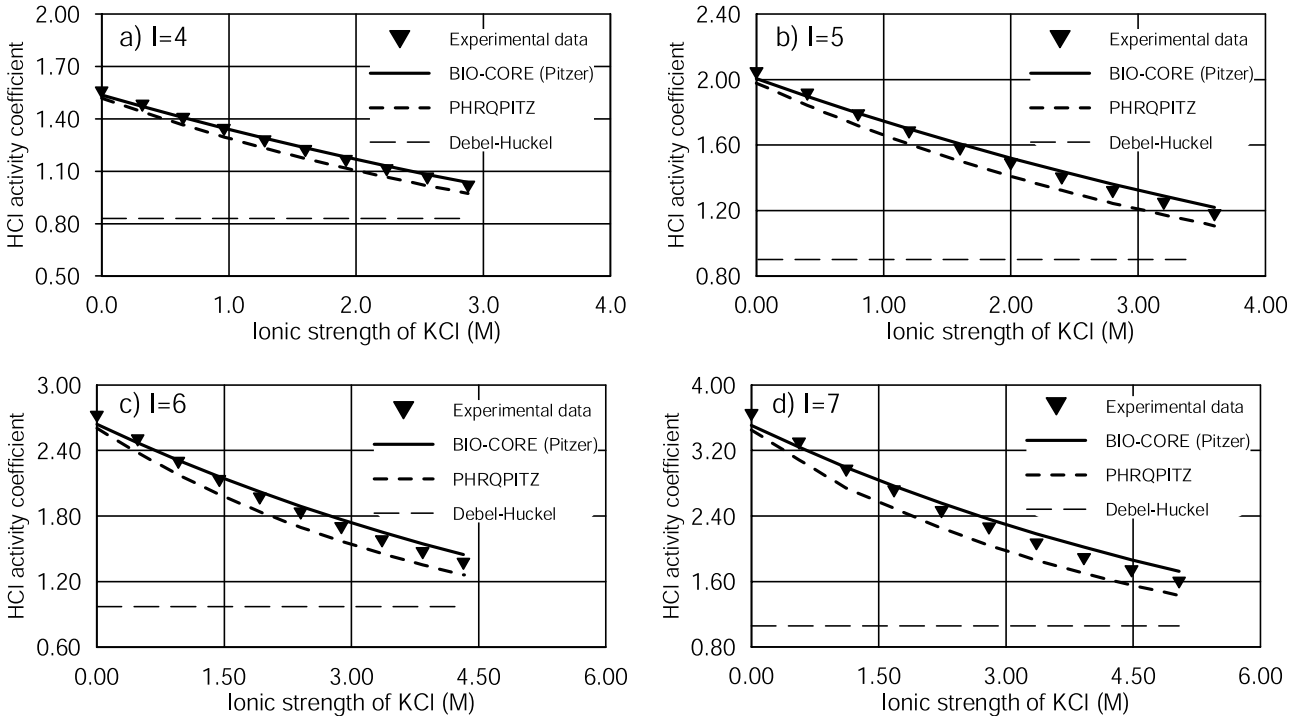

Figure 1. Comparison of the measured and the calculated mean ionic activity coefficients of HCl in an HCl-$BaCl_2$-KCl-H_2O system as a function of the concentration of KCl for total ionic strength of 4, 5, 6, and 7 M, respectively.

thermo-physical-chemical-microbial processes is considered, including aqueous complexations, acid-base, redox, mineral dissolution/precipitation, ionic exchanges, sorptions, and microbial metabolisms. The coupling between the geochemical system and the microbial ecosystem is also considered. Reactions among aqueous chemical species and mass transfer between different phases can be treated under either local equilibrium or kinetic constrains. Fluid flow is considered in variable saturated media driven by gravity and capillary forces. Heat flow is accounted for by conduction and convection. Solute transport processes considered are advection, molecular diffusion, and hydrodynamic dispersion.

[17] A two-dimensional Galerjin finite element method was used for spatial discretization. The program uses a sequential iteration approach (SIA) [*Yeh and Tripathi*, 1991] for solving the coupled system of fluid and heat flow, solute transport, and biogeochemical reactions. The SIA uses the following sequence: water flow, heat transfer, solute transport, equilibrium chemical reactions, kinetic chemical reactions, and microbial metabolisms. Solute transport is solved component to component. The biogeochemical reaction system is solved on a node-by-node basis, using the Newton-Raphson iteration method. The sequences are iteratively solved until a prescribed convergence criterion is satisfied. Full details on numerical methods are given by *Zhang* [2001], *Samper et al.* [2000], and *Xu et al.* [1999].

4. Database for the Pitzer Ion Interaction Parameters

[18] A database for Pitzer ion interaction model parameters is attached to the program, along with the existing thermodynamic and kinetic databases. The parameters of the Pitzer model are usually obtained from laboratory experiments through electromotive force (Emf) and isopiestic measurements for binary or ternary electrolytes [*Pitzer*, 1991]. *Pitzer and Mayorga* [1973] and *Pitzer* [1991] summarized a number of parameter values at 25°C for major ions. An extensive literature review of the Pitzer ion interaction parameters for many inorganic salts has been done by *Plummer et al.* [1988] in the documentation of PHRQPITZ. The values of Pitzer parameters in the database of BIO-$CORE^{2D}$ remain mostly the same as those used in PHRQPITZ. For some ions, virial parameters were taken from other literature. For example, to model the evolution of aqueous alkaline solutions at high ionic strength, we included special alkaline ions and species, based on recent literature. In particular, virial parameters for the following four systems were added: (1) polymerized silica species of high ionic strength at ambient temperature (22°–25°C) [*Felmy et al.*, 2001]; (2) sodium phosphate species in Na-PO_4-HPO_4-OH-H_2O system and their temperature dependences obtained from *Weber* [2000]; (3) the sodium aluminosilicate species in Na-$Al(OH)_4$-SiO_3-OH-CO_3-SO_4-HS-Cl system [*Park and Englezos*, 1999]; and (4) species involved in Na-H_2SiO_4 and Na-H_3SiO_4 compounds [*Hershey and Millero*, 1986].

[19] The Pitzer's virial parameters are temperature- and pressure-dependent. The ionic activity coefficients and their partial molal volumes at any given temperature are conventionally obtained by calculating Pitzer parameters and the Debye-Hückel slopes. Temperature-dependence of the virial parameters can thus be expressed using the derivative terms of enthalpies and heat capacities with respect to temperature. The first-order derivative terms of virial

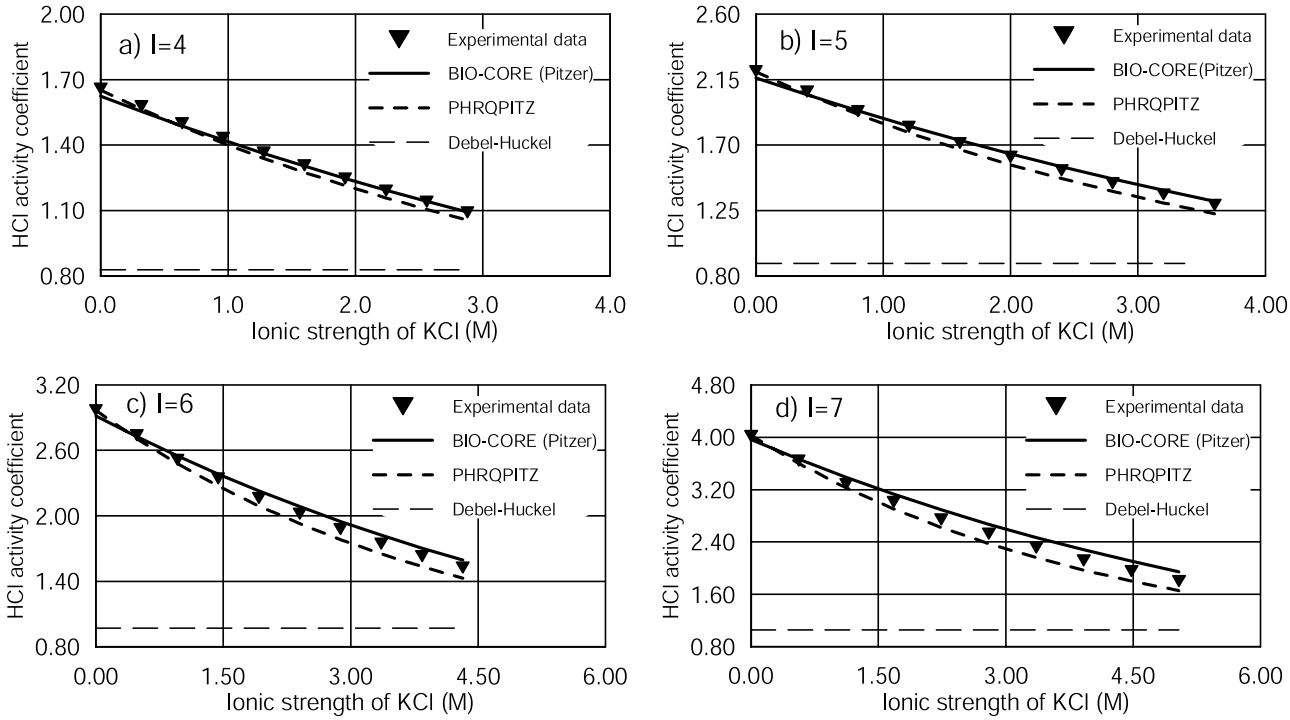

Figure 2. Comparison of the measured and the calculated mean ionic activity coefficients of HCl in an HCl-NaCl-KCl-H_2O system as a function of the concentration of KCl for total ionic strength of the solution at 4, 5, 6, and 7 M, respectively.

parameters with respect to temperature for the selected inorganic compounds at 298.15 K were reported [*Silvester and Pitzer*, 1978].

[20] Although a number of studies in the past decade, have focused on the thermodynamic properties of concentrated aqueous solutions [e.g., *Pitzer*, 1991], no acceptable model currently exists for correlating the available data for solutions over a sufficiently large temperature range. Instead, individual and arbitrary equations have often been used to describe this dependence, based on interpolations and extrapolations of the experimental data. The interpolation and extrapolation equations for various thermodynamic properties of aqueous solutions, for binary and ternary systems and for multiple-component mixtures within the Pitzer formulation, have been reported in many papers [*Harvie et al.*, 1984; *Pabalan and Pitzer*, 1989; *Harvie et al.*, 1987; *Moller*, 1988; *Greenberg and Moller*, 1989; *Monnin*, 1989, 1994; *Pitzer*, 1991; *Weber et al.*, 1999]. These authors utilized a variety of activity data, enthalpy data, and heat capacities to construct comprehensive equations over the temperature range of 0 to 250°C. For example, *Pabalan and Pitzer* [1989] fitted their experimental results with equations using more than 20 adjustable parameters. *Moller* [1988] and *Greenberg and Moller* [1989] used an equation with 10 adjustable parameters to describe the temperature-dependent parameters [*Azaroual et al.*, 1997]. In the present paper, we use the following algebraic equation:

$$P(T) = P_{T_0} + a_1(T - T_0) + a_2\left(\frac{1}{T} - \frac{1}{T_0}\right) + a_3 \ln\left(\frac{T}{T_0}\right) + a_4\left(T^2 - T_0^2\right) \quad (7)$$

where $P(T)$ represents Pitzer parameters $\beta^{(0)}$, $\beta^{(1)}$, $\beta^{(2)}$, and C^{Φ}_{MX} at temperature T (absolute temperature); T_0 is the reference temperature (298.15 K used in the database). The polynomial coefficients a_1, a_2, a_3, and a_4 in equation (7) are adjustable fitting coefficients according to experimental data. P_{T_0} is the Pitzer virial parameters at the reference temperature. Equation (7) is valid in a temperature range of 0°–100°C; extrapolation of these data to higher temperature and mixed solutions may be unreliable [*Lu et al.*, 1996]. The data in this database were verified against experimental measurements for ionic strength range of 0–7 M. (Selected test cases are presented in section 5.) The data can be applicable to solutions with higher ionic strength; however, a model calibration is needed to confirm the availability of the data where dealing with solutions with ionic strength higher than 7 M.

[21] The dependency of the Pitzer parameters on pressure is not considered in the present model because (1) within the normal natural pressure range (100 kPa ± 50 kPa under laboratory conditions and less than 1000 kPa under natural groundwater system conditions), the dependency of the Pitzer virial parameters on pressure is less significant than that on temperature within the possible temperature range under laboratory and natural conditions (−60° to +100°C); and (2) fewer experimental data are available for the pressure dependency.

5. Tests of the Model

[22] Two cases are presented here to test the Pitzer-type ion interaction model implemented in BIO-CORE^{2D}. The extensive tests and validations of BIO-CORE^{2D} dealing with reactive biogeochemical transport problems

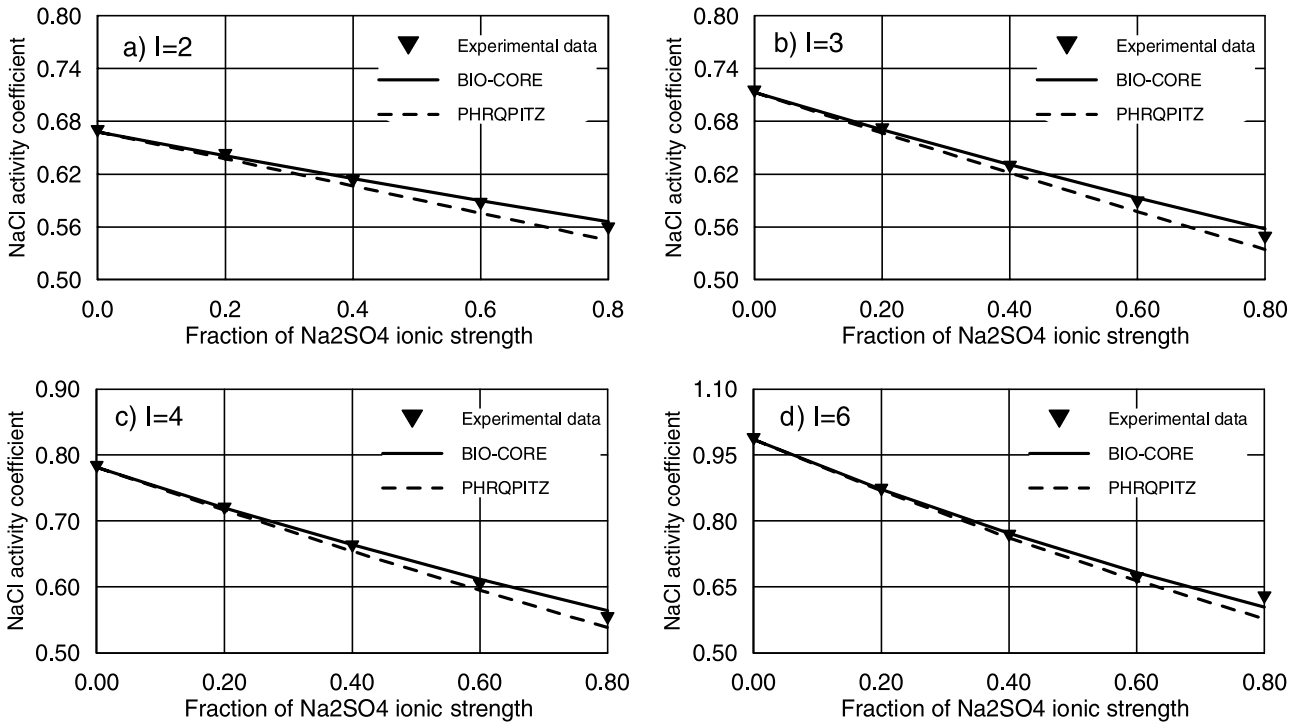

Figure 3. Comparison of the measured and the calculated mean ionic activity coefficients of NaCl in a NaCl-Na_2SO_4-H_2O system as a function of the fraction of Na_2SO_4 ionic strength at 25°C and total solution ionic strength of 2, 3, 4, and 6 M, respectively.

have been previously performed [*Zhang*, 2001] against analytical solutions of *Sun et al.* [1999] and numerical solutions from other codes [*Zhang*, 2001], which are beyond the scope of this paper.

5.1. Activity Coefficient of Hydrochloric Acid in Concentrated Electrolyte Solutions

[23] The measured mean activity coefficients of hydrochloric acid in ternary aqueous solutions of HCl-NaCl-KCl-H_2O and HCl-$BaCl_2$-KCl-H_2O, at constant total ionic strengths of 4, 5, 6, and 7 mol/kg and at temperature of 298.15 K, have been previously reported [*Jiang*, 1996]. Here we use these measured data to test our Pitzer-type ion interaction model.

[24] To maintain a constant value for the total ionic strength of the system, the experiments compensate for the changes in concentration of HCl by changes in concentration of KCl. Figure 1 shows variations of the mean activity coefficient of HCl in an HCl-$BaCl_2$-KCl-H_2O system as a function of concentrations of KCl at 298.15 K. Similarly, Figure 2 presents variations of the mean activity coefficient of HCl in an HCl-NaCl-KCl-H_2O system as a function of concentrations of KCl at 298.15 K. In Figure 2, NaCl replaces the $BaCl_2$ of Figure 1. Excellent agreement between the experimental data and our model predictions was obtained. At higher ionic strength (6–7M), our model predictions slightly deviate from the experimental data, but can still be considered well matched to that data. Figures 1 and 2 also indicate that our model predictions are better than those from PHRQPITZ [*Plummer et al.*, 1988]. On the other hand, large discrepancies were observed between Debye-Hückel modeling results and the experimental data. It can be clearly seen that the Debye-Hückel model is unable to describe the variation in individual ionic activity, because the total ionic strength remains constant in the system.

5.2. Activity Coefficient of NaCl in Aqueous Solutions at Varying Temperatures

[25] To verify the temperature dependence of the model equations and the parameters, test cases against experimental measurements performed at different temperatures are necessary. *Galleguillos-Castro et al.* [1999] conducted a thermodynamic study on NaCl-Na_2SO_4 aqueous solution

Table 1. Experimental Conditions and Hydrological Parameters Used in the Model

	Description
Column size	0.25 m (length) × 0.038 m (diameter), spatial discretization with Δx = 0.0025 cm
Filled material	quartz (mass fraction f_m > 90%, average diameter of particles, φ = 0.2 mm, surface area, A_s = 50,000 dm^2/dm^3 porous medium); density, ρ = 1.72kg/L; porosity, ϕ = 0.4; initial saturation, S_0 = 25%; residual saturation, S_r = 7%.
Flow parameters	flow rate = 0.0432 L/d; permeability = 0.64 m/d; van Genuchten m = 0.731; van Genuchten α = 9.0 m^{-1}.
Transport parameters	diffusion coefficient, $D_0 = 10^{-9}$ m^2/s; dispersivity, α_L = 0.002 m.

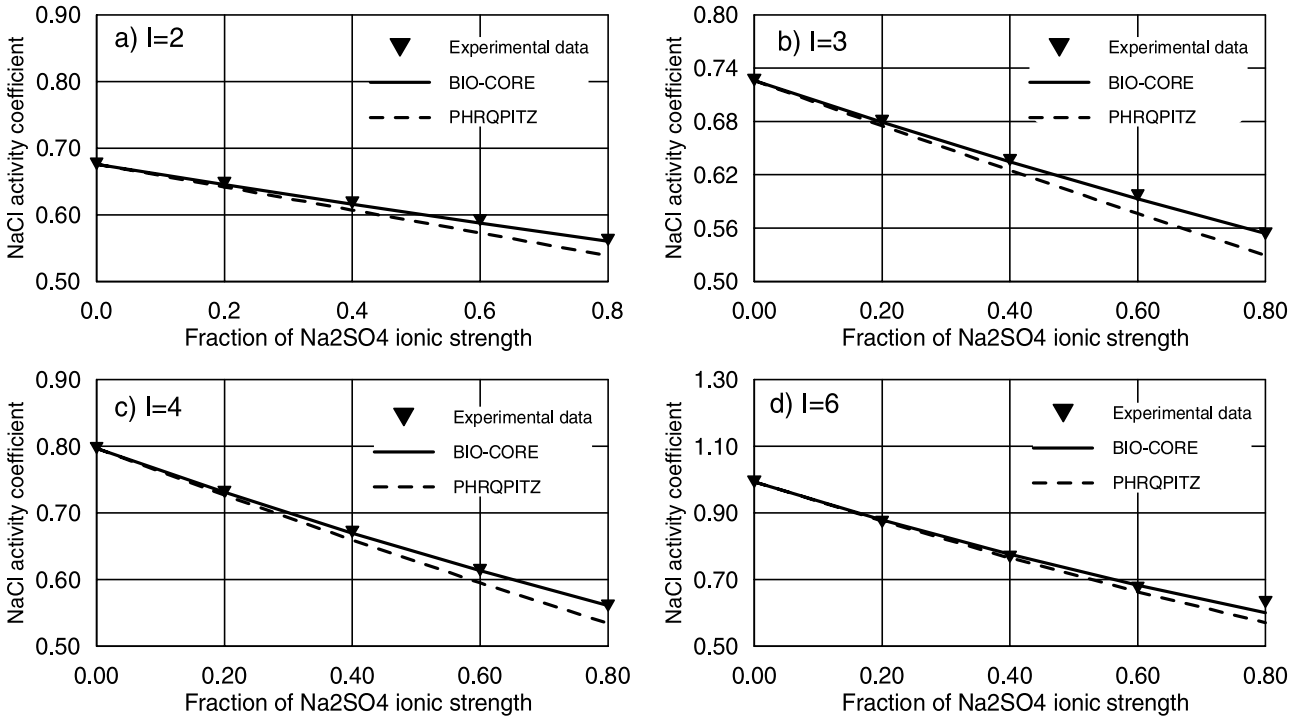

Figure 4. Comparison of the measured and the calculated mean ionic activity coefficients of NaCl in a NaCl-Na_2SO_4-H_2O system as a function of the fraction of Na_2SO_4 ionic strength at 45°C and total solution ionic strength of 2, 3, 4, and 6 M, respectively.

under four different temperatures. Using the same ion interaction parameters reported in their paper, we calculated the mean activity coefficients of NaCl at two temperatures. Results are presented in Figure 3 for the case at 25°C and Figure 4 for the case at 45°C. The total ionic strength was remained constant in four different cases, at 2, 3, 4, and 6 M. Therefore the mean activity coefficient of NaCl changed according to the ionic strength ratio of NaCl and Na_2SO_4. The measured data of the mean activity coefficients of NaCl at two temperatures were well reproduced by the BIO-CORE^{2D} simulations (Figures 3 and 4). Slight differences between model results and experimental data are within the uncertainties of analytical techniques. Once again, our model results fit experimental data better than those from PHRQPITZ.

6. Application to the Leakage of the Highly Concentrated Radioactive Waste Fluid at Hanford

[26] At the Hanford site, highly alkaline waste fluids (often >5 M of $NaNO_3$) are stored in 149 single-shell and 28 double-shell underground tanks. Sixty-seven single-shell tanks have been identified as leaking and have released an estimated 1 million gallons of mixed waste solutions into the vadose (unsaturated) zone sediments underneath the tanks. Understanding the chemistry of these saline $NaNO_3$ solutions, and how they interact with sediments, is important for assessing the contaminant migration and developing remedial actions. For this purpose, a laboratory column experiment was performed using sediment from the Hanford site and a synthetic aqueous solution similar to the Hanford tank fluid [*Wan et al.*, 2004a]. The experiments and modeling were focused on the leaking process; the dilution by rainwater infiltration after the leaking processes [*Lichtner et al.*, 2004] was not considered. One pore volume of simulated waste fluid was injected into the sediment columns at our best estimated flow rate. The historical data on leaking rates, different from tank to tank and time to time, were not available. Here we briefly report on the experimental results and simulations to illustrate and validate our Pitzer-type reactive geochemical transport model.

6.1. Problem Setup

[27] The sediment used in this experiment consists of more than 90% of fine quartz sand and clays with a cation

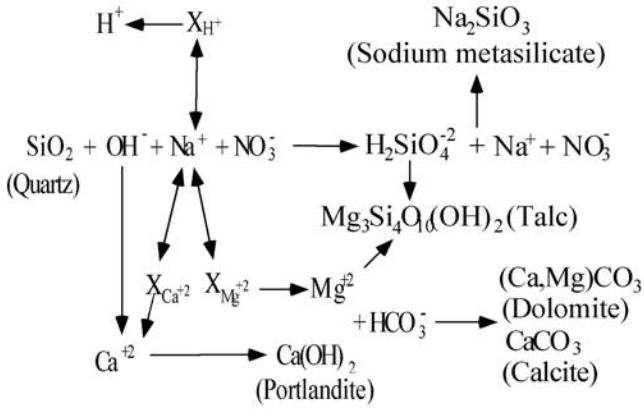

Figure 5. Schematic illustration of the major geochemical processes taking place in the column filled up with sediment from the Hanford site when injecting the simulated Hanford high-alkaline tank waste fluid. $X_{Ca^{+2}}$, $X_{Mg^{+2}}$, and X_{H^+} represent the exchangeable cations.

Table 2. Summary of the Chemical System Considered in the Model[a]

Components	H_2O	Na^+	Ca^{+2}	Mg^{+2}	NO_3^-	HCO_3^-	SO_4^{-2}	$SiO_{2(aq)}$	pH
Concentrations in the column pore water, M/L	1.0[b]	1.18×10^{-03}	4.48×10^{-04}	2.12×10^{-04}	1.00×10^{-10}	1.38×10^{-03}	5.60×10^{-04}	1.07×10^{-04}	8.22
Concentrations of the injected fluid, M/L	1.0[b]	5.0	1.0×10^{-10}	1.0×10^{-10}	4.0	1.0×10^{-10}	1.0×10^{-10}	1.0×10^{-10}	13.4

	Reactions	Log (K)
Aqueous complexes		
OH^-	$OH^- = H_2O - H^+$	1.3997E+01
CO_3^{-2}	$CO_3^{-2} = HCO_3^- - H^+$	1.0339E+01
HSO_4^-	$HSO_4^- = SO_4^{-2} + H^+$	−1.9791E+00
$H_3SiO_4^-$	$H_3SiO_4^- = SiO_{2(aq)} + 2H_2O - H^+$	9.8120E + 00
$H_2SiO_4^{-2}$	$H_2SiO_4^{-2} = SiO_{2(aq)} + 2H_2O - 2H^+$	2.2912E+01
$NaOH_{(aq)}$	$NaOH_{(aq)} = Na^+ + H_2O - H^+$	1.4180E+01
$NaHCO_{3(aq)}$	$NaHCO_{3(aq)} = Na^+ + HCO_3^-$	−1.5410E−01
$NaCO_3^-$	$NaCO_3^- = Na^+ + HCO_3^- - H^+$	9.8249E+00
$NaSO_4^-$	$NaSO_4^- = Na^+ + SO_4^{-2}$	−8.2000E−01
$NaHSiO_{3(aq)}$	$NaHSiO_{3(aq)} = Na^+ + SiO_{2(aq)} + H_2O - H^+$	8.3040E+00
$NaH_3SiO_{4(aq)}$	$NaH_3SiO_{4(aq)} = Na^+ + SiO_{2(aq)} + 2H_2O - H^+$	8.6616E+00
$CaOH^+$	$CaOH^+ = Ca^{+2} + H_2O - H^+$	1.2850E+01
$CaNO_3^+$	$CaNO_3^+ = Ca^{+2} + NO_3^-$	−7.0000E−01
$CaHCO_3^+$	$CaHCO_{3(aq)}^+ = Ca^{+2} + HCO_3^-$	−1.0467E+00
$CaCO_{3(aq)}$	$CaCO_{3(aq)} = Ca^{+2} + HCO_3^- - H^+$	7.1880E+00
$CaSO_{4(aq)}$	$CaSO_{4(aq)} = Ca^{+2} + SO_4^{-2}$	−2.1111E+00
$Ca(H_3SiO_4)_{2(aq)}$	$Ca(H_3SiO_4)_{2(aq)} = Ca^{+2} + 2SiO_{2(aq)} + 4H2O - 2H^+$	1.5053E+01
$MgOH^+$	$MgOH^+ = Mg^{+2} + H_2O - H^+$	1.1787E+01
$MgHCO_3^+$	$MgHCO_3^+ = Mg^{+2} + HCO_3^-$	−1.0357E+00
$MgCO_{3(aq)}$	$MgCO_{3(aq)} = Mg^{+2} + HCO_3^- - H^+$	7.3604E+00
$MgSO_{4(aq)}$	$MgSO_{4(aq)} = Mg^{+2} + SO_4^{-2}$	−2.4117E+00
$Mg(H_3SiO_4)_{2(aq)}$	$Mg(H_3SiO_4)_{2(aq)} = Mg^{+2} + 2SiO_{2(aq)} + 4H2O - 2H^+$	1.3723E+01
$CO_{2(aq)}$	$CO_{2(aq)} = HCO_3^- - H^+$	−6.3375E+00
Minerals		
Quartz	Quartz $\Rightarrow SiO_{2(aq)}$	rate = 5×10^{-8} $[OH^-]^{0.5}$ mol/s/dm^2
Portlandite ($Ca(OH)_2$)	portlandite = $Ca^{+2} + 2H2O - 2H^+$	2.2555E+01
Sodium silicate (Na2sio3)	sodiunmsilicate = $2Na^+ + SiO_{2(aq)} + H_2O - 2H^+$	2.2241E+01
Talc	talc = $3Ca^{+2} + 4SiO_{2(aq)} + 4H2O - 6H^+$	2.1138E+01
Dolomite	dolomite = $Ca^{+2} + Mg + 2HCO_3^- - 2H^+$	2.5135E+00
Calcite	calcite = $Ca^{+2} + HCO_3^- - H^+$	1.9330E+00

Exchangeable Cations	CEC, 10 meq/100 g solid	Equilibrium Constant
H^+ (master)	0.00027	1
Na^+	0.02023	0.99
Ca^+	0.75500	0.20
Mg^+	0.22450	0.40

[a]Read 1.3997E+01 as 1.3997×10^1.
[b]The water concentration was numerically assumed 1.0 for the initial concentration and is later calculated in the model based on mass balance.

exchange capacity (CEC) of 10 meq/100 g and moisture content of 7%. An electrolytic fluid of 4 mol/L of $NaNO_3$ and 1 mol/L of NaOH, with an ionic strength of 5 M, was injected into the bottom of the column. The effluent fluid was collected at the top. A constant injection rate of 0.0432 L/d was applied. The injection led to the bottom saturating first, with the wetting front gradually moving upward. Fluid outflow from the top was observed at approximately 0.5 pore volume, with the displaced native soil water at the front.

[28] The experimental conditions and parameters of fluid flow and chemical transport are listed in Table 1. Permeability, porosity, and saturation were measured during the experiment setup; more details are given by *Wan et al.* [2004b]. Because of the small size and the relatively small flow rate, hydraulic dispersion was expected to play a limited role, and thus the dispersivity was assigned a very small value of 0.002 m. A value of 10^{-9} m^2/s for diffusion was used in the simulation. The bottom of the column was treated as flux boundary for both fluid flow and chemical transport, while the top was open for the fluid outflowing.

[29] The pH and the concentrations in the effluent fluid provide information about the processes taking place inside the column while the fluid is in contact with the sediment. The pH breakthrough especially reflects the combined effect of a number of geochemical processes. The very high pH in the influent fluid was first lowered by quartz dissolution, cation exchange (released H^+ from the sediment), and

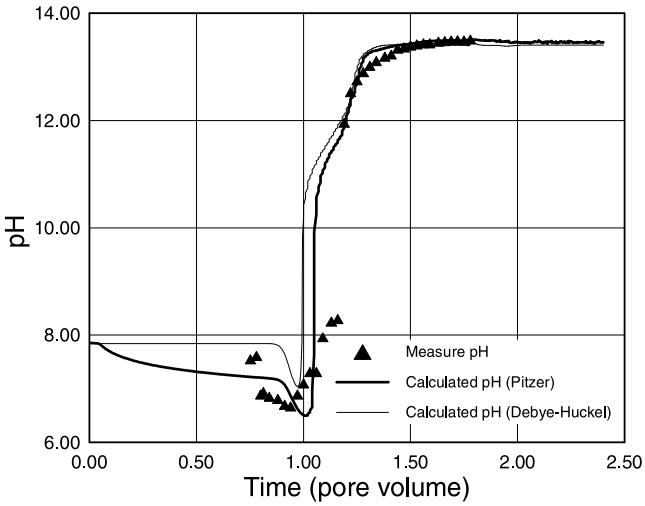

Figure 6. Simulated pH of the effluent fluid compared to measured data.

precipitation of calcite, dolomite, and talc. After a complete washout of the exchangeable cation, the pH recovered. Finally, the previously precipitated calcite and dolomite were dissolved again and washed out, while the quartz kept dissolving.

[30] Major geochemical processes considered in the simulation are shown in Figure 5. Aqueous species, minerals, exchangeable cations, and some reaction parameters are summarized in Table 2. A total of nine aqueous component species and 23 aqueous complexes were considered. The simulations considered six minerals: quartz, portlandite, sodium silicate, talc, dolomite, and calcite. Quartz was kinetics constrained; the dissolution rate is formulated as rate = $5 \times 10^{-8}[OH^-]^{0.5}$ mol/s/dm^2 [*Wan et al.*, 2004a], and the reactive surface area was estimated to be 50,000 dm^2 per dm^3 of sand. Portlandite, sodiumsilicate, talc, dolomite, and calcite were considered secondary minerals because they tend to precipitate in the initial stage of the experiment rather than to dissolve. Precipitation of these minerals was assumed at local equilibrium. Clay minerals play the role of cation exchange site, releasing Ca^{+2}, Mg^{+2}, and H^+ in exchange with Na^+ in the aqueous phase. Because of the relatively low solubility, the direct dissolution of clays is considered insignificant compared to the cation exchanges, and thus clays are not considered as primary minerals in the model. A total of four exchangeable cations, H^+, Na^+, Ca^{+2}, and Mg^{+2}, were considered. The selectivity coefficients used were taken directly from *Appelo and Postma* [1996].

Table 4. The λ Parameters of Major Aqueous Molecule-Ion Interactions Used in the Simulations (25°C)

	$CO_{2(aq)}$	$SiO_{2(aq)}$
H^+		
Na^+	0.1000E+00[a]	0.9250E − 01[b]
Ca^{+2}	0.1830E+00[a]	0.6590E−01[b]
Mg^{+2}	0.1830E+00[a]	0.6000E−01[c]
OH^-		0.1816E+00[b]
SO_4^{-2}	0.9700E−01[a]	0.2000E−01[c]
HSO_4^-	−.3000E−02[a]	
HCO_3^-		0.1500E−01
NO_3^-		0.3610E−01[c]

[a] *Plummer et al.* [1988].
[b] *Azaroual et al.* [1997].
[c] *Risacher and Clement* [2001].

6.2. Results and Discussion

[31] Figure 6 shows the simulated pH breakthrough of the effluent fluid, together with the measured values. Simulated pH using BIO-CORE^{2D} with the Pitzer model captures measured pH values better than the Debye-Hückel model. The Pitzer's ionic interaction coefficients used in the model are listed in Tables 3 and 4. Figure 7 shows the concentra-

Table 3. Virial Coefficients of the Major Ionic Pairs Used in the Simulations (25°C)

	OH^-	SO_4^{-2}	HSO_4^-	CO_3^{-2}	HCO_3^-	NO_3^-	$H_3SiO_4^-$	$H_2SiO_4^{-2}$
H^+								
β_0		0.2980E−01[a]	0.2065E+00[a]			0.1119E+00[a]		
β_1		0.0000E+00[a]	0.5556E+00[a]			0.3206E+00[a]		
β_2		0.0000E+00[a]	0.0000E+00[a]			0.0000E+00[a]		
C		0.4380E−01[a]	0.0000E+00[a]			0.1000E−02[a]		
Na^+								
β_0	0.8640E−01[b]	0.1958E−01[b]	0.4540E−01[b]	0.3990E−01[b]	0.2770E−01[b]	0.6800E−02[a]	0.4300E−01[c]	0.3200E+00[d]
β_1	0.2530E+00[b]	0.1113E+01[b]	0.3980E+00[b]	0.1389E+01[b]	0.4110E−01[b]	0.1783E+00[a]	0.2400E+00[c]	0.1300E+00[d]
β_2	0.0000E+00[b]	0.0000E+00[b]	0.0000E+00[b]	0.0000E+00[b]	0.0000E+00[b]	0.0000E+00[a]	0.0000E+00[c]	0.0000E+00[d]
C	0.4400E−02[b]	0.4970E−02[b]	0.0000E+00[b]	0.4400E−02[b]	0.0000E+00[b]	−0.7200E−03[a]	0.0000E+00[c]	0.0000E+00[d]
Ca^{+2}								
β_0	−.1747E+00[b]	0.2000E+00[b]	0.2145E+00[b]		0.4000E+00[b]	0.2108E+00[b]		
β_1	−.2303E+00[b]	0.3197E+01[b]	0.2530E+01[b]		0.2977E+01[b]	0.1409E+01[b]		
β_2	−.5720E+01[b]	−.5424E+02[b]	0.0000E+00[b]		0.0000E+00[b]	0.0000E+00[b]		
C	0.0000E+00[b]	0.0000E+00[b]	0.0000E+00[b]		0.0000E+00[b]	−.2014E−01[b]		
Mg^{+2}								
β_0		0.2210E+00[b]	0.4746E+00[b]		0.3290E+00[b]	0.3670E+00[e]		
β_1		0.3343E+01[b]	0.1729E+01[b]		0.6072E+00[b]	0.1580E+01[e]		
β_2		−.3723E+02[b]	0.0000E+00[b]		0.0000E+00[b]	0.0000E+00[e]		
C		0.2500E−01[b]	0.0000E+00[b]		0.0000E+00[b]	0.2060E−01[e]		

[a] *Pitzer* [1991].
[b] *Plummer et al.* [1988].
[c] *Hershey and Millero* [1986].
[d] *Bickmore et al.* [2001].
[e] *Risacher and Clement* [2001].

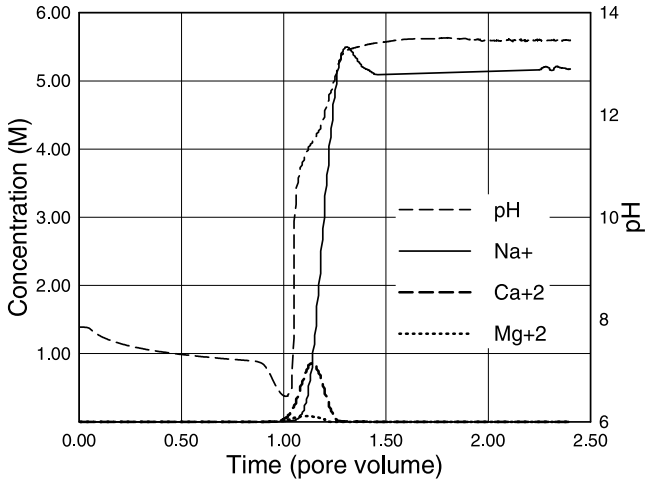

Figure 7. Breakthrough curves calculated for concentrations of Na^+, Ca^{+2}, Mg^{+2}, and pH of the effluent fluid.

tion breakthrough for Na^+, Ca^{+2}, and Mg^{+2}. The high concentration of Na^+, NO_3^-, and OH^- in the injected water causes a monotonic increase in the concentration of these components inside the column and also over time in the effluent. Na^+ in the liquid phase replaces the exchangeable Ca^{+2}, Mg^{+2}, and H^+ in the solid phase, leading to increases of Ca^{+2}, Mg^{+2}, and H^+ concentrations in the liquid phase. Peaks of Ca^{+2} and Mg^{+2} concentrations caused by these processes, as well as the decrease of pH (lower than the background value), can be clearly seen in Figure 7. Although the concentrations of Ca^{+2} and Mg^{+2} were not measured in this experiment, the simulated trends were observed in similar laboratory experiments [*Wan et al.*, 2004b].

[32] The injected fluid has very low concentrations of Ca^{+2}, Mg^{+2}, and H^+, and thus dilutes the solution after the exchangeable Ca^{+2}, Mg^{+2} and H^+ on the exchange site are washed out. This causes a decrease in Ca^{+2} and Mg^{+2} concentrations, and a pH increase behind the wetting front (Figure 7). The pH is also constrained by mineral dissolution and precipitation. Quartz initially present in the column dissolves very quickly under these high alkalinity conditions. The concentration of aqueous silica sharply increases just behind the wetting front. Consequently, talc precipitates at the point where the aqueous silica front mixes with the Mg^{+2} peak. Dolomite and calcite also precipitate in the same manner at the point where Mg^{+2} and Ca^{+2} peaks mix with the injected HCO_3^-.

[33] Figures 8 and 9 show mineral precipitation and dissolution trends inside the column. Precipitation of portlandite, sodiumsilicate, talc, dolomite, and calcite removes OH^- from the solution and decreases pH. The complete exhausting of exchangeable $Ca^{+2}$and Mg^{+2} behind the plume front results in the early precipitated talc, dolomite, and calcite to be dissolved again (to different extents) (Figure 9). Calcite and dolomite were completely dissolved behind the wetting front (Figure 9). Talc also dissolves behind the wetting front, but a significant amount of the earlier precipitation of this mineral still remains in the column (Figure 9). According to the precipitation rates of these minerals (Figure 9), we know that the dominant precipitated mineral phase is talc, because the continuous dissolution of quartz provides plenty of aqueous silica and makes the talc precipitation dominant for pH evolution.

6.3. Sensitivity Analyses

[34] The major geochemical processes in this application are cation exchange, kinetic dissolution of quartz, and precipitation of calcium and magnesium minerals. Parameter values involved in these processes may span a large range under the conditions tested. To identify the main processes affecting the plume development of alkaline solution and the possible range of key parameters, three sensitivity simulations were performed.

[35] The first sensitivity simulation excluded mineral dissolution/precipitation. The results of this simulation (Figure 10) show that the simulated pH is initially low and remains at a constant background value. Shortly after one pore volume, the pH quickly reaches the level of the injected-fluid pH. The decreasing region of pH (lower than the background level) observed at around one pore volume becomes very slight (about 15% of the observed pH drop-down magnitude). The peaks of Ca^{+2} and Mg^{+2} concentrations resulting from cation exchange are elevated (not shown). This simulation cannot reproduce the measured pH breakthrough. The dissolution and precipitation of those minerals are very important because, first, quartz dissolution provides aqueous silica to precipitate talc with the released Mg^{+2} from the exchange site, and sodium silicate with the injected Na^+. These precipitations remove OH^-, causing a pH decrease. Second, the released Ca^{+2} and Mg^{+2} from the exchange site are also precipitated to form calcite, and dolomite together with the HCO_3^- initially appearing in the sand moisture; and these precipitations also remove OH^-, causing pH decrease. Third, the released Ca^{+2} from the exchange site directly precipitated with OH^- to form portlandite, causing pH decrease. If there were no quartz dissolution, there would be no aqueous silica, and consequently, talc and sodium silicate would not precipitate. If there were no precipitation of talc, sodium silicate, calcite,

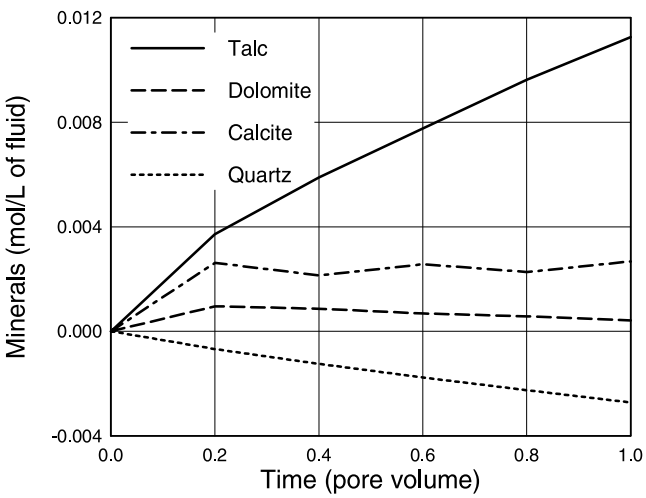

Figure 8. Simulated accumulative precipitations (positive) of talc, dolomite, calcite, and dissolution (negative) of quartz at different times (spatially maximum values). Precipitations of sodium silicate and portlandite are minor (not shown).

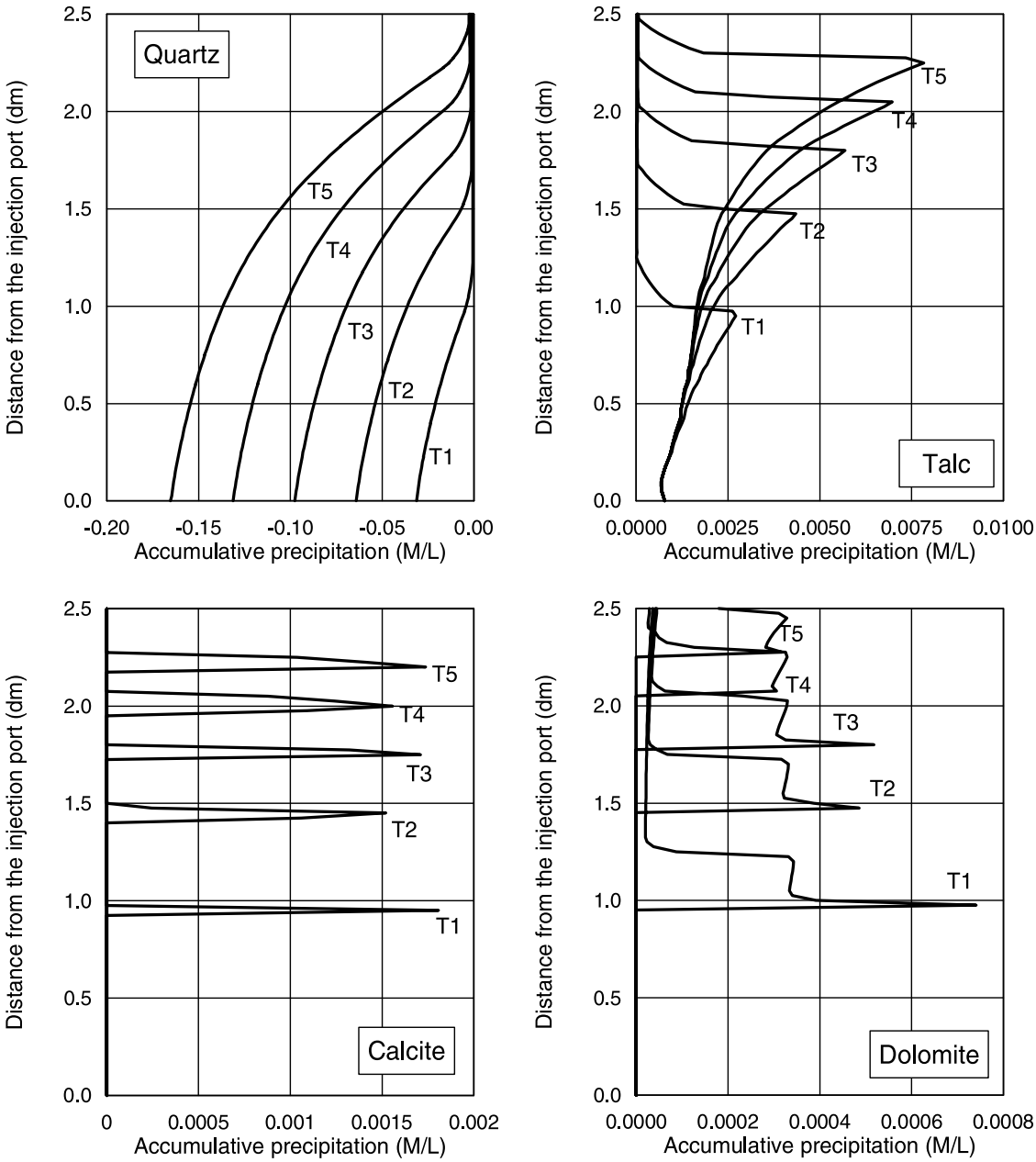

Figure 9. Simulated accumulative precipitation (positive) of talc, dolomite, calcite, and dissolution (negative) of quartz inside the column at different times: T1 corresponds to 0.2 pore volume, T2 corresponds to 0.4 pore volume, T3 corresponds to 0.6 pore volume, T4 corresponds to 0.8 pore volume, and T5 corresponds to 1.0 pore volume. Precipitations of sodium silicate and portlandite are minor (not shown).

and dolomite, OH^- would not be removed, and the pH would not decrease so severely.

[36] In the second sensitivity simulation, we took away the cation exchange reactions. The simulated pH is also plotted in Figure 10. Results show that the measured diminishing pH region that was reproduced in the base case simulation (Figure 6) disappears, and the peaks of Ca^{+2} and Mg^{+2} concentrations (measured by *Wan et al.* [2004b] and reproduced in the base case simulation, as can be seen in Figure 7) also disappear (not shown), because no H^+ is released to lower the pH, and no Ca^{+2} and Mg^{+2} are released to precipitate minerals and remove OH^- from the aqueous phase.

[37] In the third sensitivity simulation, we used a kinetic rate constant of quartz dissolution decreased by one order of magnitude. The results show that the simulated pH evolution is highly sensitive to the kinetic rate of quartz dissolution. The smaller kinetic rate leads to a higher pH before one pore volume and a smaller pH drop after one pore volume. This is because the smaller dissolution rate causes a lower concentration of aqueous silica and less precipitation of talc and sodium silicate. Consequently, a smaller amount of OH^- was removed and a higher pH was obtained (Figure 10). Thus the dissolution of quartz and the precipitation of other minerals are essential in this geochemical system. However, the kinetic rate of quartz

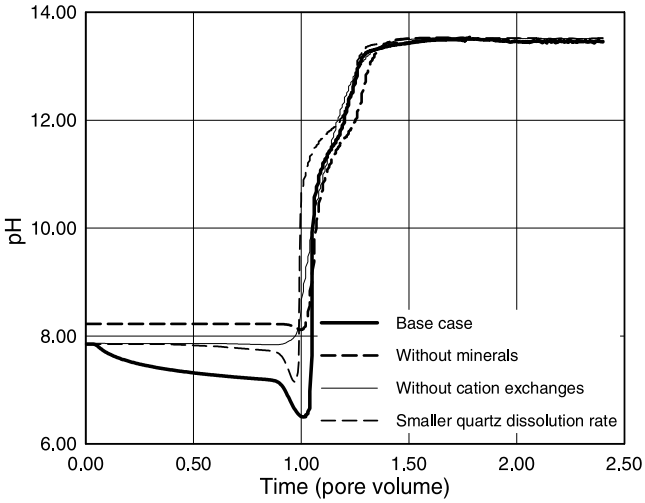

Figure 10. Sensitivity analyses of calculated pH with respect to mineral dissolution/precipitation, cation exchanges, and smaller kinetic rate of quartz dissolution (one order of magnitude).

dissolution strongly depends on the specific surface area and solution chemistry [*Rimstidt and Barnes*, 1980; *Dove*, 1994; *Rimstidt*, 1997]. The surface area of quartz is a sediment-type-dependent parameter, requiring independent estimation or measurement.

[38] Sensitivity simulations indicate that pH is strongly influenced by cation exchange and mineral dissolution and precipitation. The sensitivity analysis results also suggest that the high alkaline solution leaking into a subsurface environment could induce strongly coupled geochemical processes, controlling the development of the waste plume.

7. Conclusions

[39] We have incorporated the Pitzer ion interaction model into an existing reactive biogeochemical transport code, BIO-CORE^{2D}, to simulate the coupled transport and chemical reactions of aqueous solutions at high ionic strength taking place in natural and engineered systems. The model was tested against two reported cases with observation data. The measured data of mean activity coefficients were well reproduced by BIO-CORE^{2D}. Our model results match experimental data better than those simulated using PHRQPITZ.

[40] The developed model was applied to simulate a laboratory column experiment, injecting a highly alkaline (4 M $NaNO_3$ + 1 M NaOH) solution into sediment from the Hanford site to simulate the leaking processes of the highly alkaline solutions stored at the site. We found that with the Pitzer-type geochemical model implemented in BIO-CORE^{2D}, simulation results capture the measured pH values better than those using the Debye-Hückel model. The simulation results indicate that exchanges of the injected Na^+ with the exchangeable H^+, Ca^{+2}, and Mg^{+2} on the exchange site; quartz dissolution; and talc, dolomite, and calcite precipitation are strongly coupled. Quartz dissolution provides a source of aqueous silica; the injected Na^+ replaces Ca^{+2}, Mg^{+2}, and H^+ in the solid phase (releasing them into the solution); and the precipitation of talc, calcite, dolomite, sodium silicate and portlandite remove OH^- from the solution, leading to pH decrease at about 1 pore volume. All these reactions contribute to pH evolution. Sensitivity analyses indicated that the major (~85%) contribution to the pH decrease was from the precipitation of calcium and magnesium minerals, predominantly talc, which removes OH^-. The H^+ directly released (from the exchange site) had little effects on the pH decrease. However, the Ca^{+2} and Mg^{+2} were also sourced from the solid phase through cation exchanges with Na^+.

Appendix A: Debye-Hückel Formula for Activity Coefficient

[41] For dilute solutions (ionic strength smaller than 1 M), values of the activity coefficients are usually calculated according to the extended Debye-Hückel formula, which is expressed as

$$\log \gamma_i = -\frac{Az_1^2 (I)^{\frac{1}{2}}}{1 + Ba_i (I)^{\frac{1}{2}}} + bI \tag{A1}$$

where I is the ionic strength of the solution; z_i and a_i are the electric charge and the ionic radius of ith aqueous species, respectively; A and B are constants that depend on the temperature and dielectric constant of water, and b is a constant determined from fitting experimental data. The values of A, B, and b at different temperatures are tabulated by *Helgeson and Kirkham* [1974]. The value of the ionic strength is calculated as

$$I = \frac{1}{2} \sum_{i=1}^{N_T} c_i z_i^2 \tag{A2}$$

[42] The activity of water can be calculated according to *Garrels and Christ* [1965] as

$$a_{H_2O} = 1 - 0.018 \sum_{i=2}^{N_T} c_i \tag{A3}$$

where i includes all the species in solution except water.

Appendix B: Definition of Coefficients in the Pitzer Virial Equations

[43] Coefficient Z, in front of C_{ca} in equation (2) is given by

$$Z = \sum_{k=1}^{N} |z_k| m_k \tag{B1}$$

where z_k and m_k are the electrical charge and molality of the kth species, respectively. A^Φ is one third of the Debye-Hückel limiting slope and is temperature-dependent, with a value of 0.392 at 25°C and 1 atm. The temperature dependence of A^Φ, according to *Clegg and Whitfield* [1991], is given by

$$A^\Phi = \begin{cases} 0.13422(0.0368329T - 14.62718 \ln T \\ \quad -\dfrac{1530.1474}{T} + 80.40631) \quad (-60°C \le T \le 0°C) \\ 0.13422\left(4.1725332 - 0.1481291\sqrt{T} + 1.5188505 \times 10^{-5} T^2\right. \\ \quad \left. -1.8016317 \times 10^{-8} T^3 + 9.3816144 \times 10^{-10} T^{3.5}\right) \quad (-0°C \le T \le 100°C). \end{cases} \tag{B2}$$

where T is absolute temperature.

[44] The modified Debye-Hückel term used in equations (3) and (4), are defined as

$$F = -A^{\Phi}\left(\frac{\sqrt{I}}{1+1.2\sqrt{I}} + \frac{2}{1.2}\ln\left(1+1.2\sqrt{I}\right)\right) + \sum_{c=1}^{N_c}\sum_{a=1}^{N_a} m_c m_a B'_{ca} \tag{B3}$$

[45] All Pitzer virial coefficients, B^{Φ}_{ca}, B_{MX} (representing B_{Ma} and B_{cX}), B'_{MX} (representing B'_{Ma} and B'_{cX}), α_{MX}, and C_{MX} (representing C_{Ma}, C_{cX} and C_{ca}) in equations (2), (3), and (4) are defined as:

$$B^{\Phi}_{ca} = \beta^{(0)}_{MX} + \beta^{(1)}_{MX} e^{-\alpha_{MX}\sqrt{I}} + \beta^{(2)}_{MX} e^{-\alpha'_{MX}\sqrt{I}} \tag{B4}$$

$$B_{MX} = \beta^{(0)}_{MX} + \beta^{(1)}_{MX} g\left(\alpha_{MX}\sqrt{I}\right) + \beta^{(2)}_{MX} g\left(\alpha'_{MX}\sqrt{I}\right) \tag{B5}$$

$$B'_{MX} = \beta^{(1)}_{MX}\frac{g'\left(\alpha_{MX}\sqrt{I}\right)}{I} + \beta^{(2)}_{MX}\frac{g'\left(\alpha'_{MX}\sqrt{I}\right)}{I} \tag{B6}$$

[46] The function g(x) and g′(x) are given by

$$g(x) = 2\frac{(1-(1+x)e^{-x})}{x^2} \tag{B7}$$

$$g'(x) = -2\frac{\left(1-\left(1+x+\frac{x^2}{2}\right)e^{-x}\right)}{x^2} \tag{B8}$$

where x in equations (B7) and (B8) denotes $\alpha_{MX}\sqrt{I}$ or $\alpha'_{MX}\sqrt{I}$. For any salt containing a monovalent ion, $\alpha_{MX} = 2$ and $\alpha'_{MX} = 12$; for 2-2 electrolytes, $\alpha_{MX} = 1.4$ and $\alpha'_{MX} = 12$; for 3-2 and 4-2 electrolytes, $\alpha_{MX} = 2.0$ and $\alpha'_{MX} = 50$ [*Silvester and Pitzer*, 1978].

[47] The thermodynamic properties of single-salt solutions, C_{MX}, are given by:

$$C_{MX} = \frac{C^{\Phi}_{MX}}{2\sqrt{|z_M z_X|}} \tag{B9}$$

[48] Therefore defining the activity coefficients and osmotic coefficients for an aqueous solution requires estimates of $\beta^{(0)}_{MX}$, $\beta^{(1)}_{MX}$, $\beta^{(2)}_{MX}$, C^{Φ}_{MX} and λ for the appropriate solution ionic pairs. Note that λ represents λ_{nc}, λ_{na}, λ_{nM}, λ_{nX}, λ_{Nc}, and λ_{Na}. In all the above formulations, the unit of m_i, m_c, m_a and I is molality, and units of parameters $\beta^{(0)}_{MX}$, $\beta^{(1)}_{MX}$, $\beta^{(2)}_{MX}$, C^{Φ}_{MX} and λ_{nc}, λ_{na}, λ_{nM}, λ_{nX}, λ_{Nc}, and λ_{Na}, are derived.

[49] **Acknowledgments.** We thank Daniel Hawkes, Tianfu Xu, and Tetsu K. Tokunaga for internal review of the manuscript and suggestions for improvements. We also thank the anonymous WRR reviewers for their helpful comments. This work was supported by the U.S. Department of Energy under contract DE-AC03-76SF00098 with Lawrence Berkeley National Laboratory. Funding is partially from the Environmental Management Science Program.

References

Appelo, C. A. J., and D. Postma (1996), *Geochemistry, Groundwater and Pollution*, A. A. Balkema, Brookfield, Vt.

Azaroual, M., C. Fouillac, and J. M. Matray (1997), Solubility of silica polymorphs in electrolyte solutions, 1. Activity coefficient of aqueous silica from 25°C to 250°C, Pitzer's parameterisation, *Chem. Geol.*, *140*(3–4), 155–165.

Bethke, C. M. (1996), *Geochemical Reaction Modeling: Concepts and Applications*, 397 pp., Oxford Univ. Press, New York.

Bickmore, B. R., K. L. Nagy, J. S. Young, and J. W. Drexler (2001), Nitrate-cancrinite precipitation on quartz sand in simulated Hanford tank solutions, *Environ. Sci. Technol.*, *35*(22), 4481–4486.

Blowes, D. W., E. J. Reardon, J. L. Jambor, and J. A. Cherry (1991), The formation and potential importance of cemented layers in inactive sulfide mine tailings, *Geochim. Cosmochim. Acta*, *55*(4), 965–978.

Boufadel, M. C., M. T. Suidan, and A. D. Venosa (1999), A numerical model for density-and-viscosity-dependent flows in two-dimensional variably saturated porous media, *J. Contam. Hydrol.*, *37*(1), 1–20.

Clegg, S. L., and M. Whitfield (1991), Activity coefficients in natural waters, in *Activity Coefficients in Electrolyte Solutions*, 2nd ed., edited by K. S. Pitzer, pp. 279–434, CRC Press, Boca Raton, Fla.

Dougherty, R. C. (2001), Density of salt solution: Effects of ions on the apparent density of water, *J. Phys. Chem. B*, *105*(19), 4514–4519.

Dove, P. M. (1994), The dissolution kinetics of quartz in sodium chloride solutions at 25 to 300°C, *Am. J. Sci.*, *294*, 665–712.

Felmy, A. R. (1995), GMIN, a computerized chemical equilibrium program using a constrained minimization of the Gibbs free energy: Summary report, *Spec. Publ. Soil Sci. Soc. Am.*, *42*, 377–407.

Felmy, A. R., H. Cho, J. R. Rustad, and M. J. Mason (2001), An aqueous thermodynamic model for polymerized silica species to high ionic strength, *J. Solution Chem.*, *30*(6), 509–525.

Galleguillos-Castro, H. R., F. Hernandez-Luis, L. Fernandez-Merida, and M. A. Esteso (1999), Thermodynamic study of the NaCl + Na2SO$_4$ + H$_2$O system by Emf measurements at four temperatures, *J. Solution Chem.*, *28*(6), 791–807.

Garrels, R. M., and C. L. Christ (1965), *Solutions, Minerals and Equilibria*, 450 pp., W. H. Freeman, New York.

Gephart, R. E., and R. E. Lundgren (1998), *Hanford Tank Cleanup*, Battelle, Columbus, Ohio.

Gerson, A. R., and K. Zheng (1997), Bayer process plant scale: Transformation of sodalite to cancrinite, *J. Cryst. Growth*, *171*(1–2), 209–218.

Greenberg, J. P., and N. Moller (1989), The prediction of mineral solubilities in natural waters: A chemical equilibrium model for the Na-K-Ca-Cl-SO$_4$-H$_2$O system to high concentration from 0 to 250°C, *Geochim. Cosmochim. Acta*, *53*(10), 2503–2518.

Harvie, C. E., and J. H. Weare (1980), The prediction of mineral solubilities in natural waters: The Na-K-Mg-Ca-Cl-SO$_4$-H$_2$O system from zero to high concentration at 25°C, *Geochim. Cosmochim. Acta*, *44*(7), 981–997.

Harvie, C. E., N. Moller, and J. H. Weare (1984), The prediction of mineral solubilities in natural waters: The Na-K-Mg-Ca-H-Cl-SO$_4$-OH-HCO$_3$-CO$_3$-H$_2$O-system to high ionic strengths at 25°C, *Geochim. Cosmochim. Acta*, *48*(4), 723–751.

Harvie, C. E., J. P. Greenberg, and J. H. Weare (1987), A chemical equilibrium algorithm for highly nonideal multiphase systems: Free energy minimization, *Geochim. Cosmochim Acta*, *51*(5), 1045–1057.

Helgeson, H. C., and D. H. Kirkham (1974), Theoretical prediction of the thermodynamic behavior of aqueous electrolytes at high pressures and temperatures: II. Debye-Hückel parameters for activity coefficients and relative partial molal properties, *Am. J. Sci.*, *274*, 1199–1261.

Herbert, A. W., C. P. Jackson, and D. A. Lever (1988), Coupled groundwater flow and solute transport with fluid density strongly dependent upon concentration, *Water Resour. Res.*, *24*, 1781–1795.

Hershey, J. P., and F. J. Millero (1986), The dependence of the acidity constants of silicic acid on NaCl concentration using Pitzer's equations, *Mar. Chem.*, *18*(1), 101–105.

Jiang, C. (1996), Activity coefficients of hydrochloric acid in concentrated electrolyte solutions, 2. HCl + BaCl$_2$ + KCl + H$_2$O, HCl + LiCl + KCl + H$_2$O, and HCl + NaCl + KCl + H$_2$O at 298.15K, *J. Chem. Eng. Data*, *41*(1), 117–120.

Krumgalz, B. S. (2001), Application of the Pitzer ion-interaction model to natural hypersaline brines, *J. Mol. Liq.*, *91*(1), 3–19.

Lichtner, P. C. (2001), FLOTRAN user's manual, *LA-UR-01-2349*, Los Alamos Natl. Lab., Los Alamos, N. M.

Lichtner, P. C., and A. Felmy (2003), Estimation of Hanford SX tank waste compositions from historically derived inventories, *Comput. Geosci.*, *29*(3), 371–383.

Lichtner, P. C., S. Yabusaki, K. Pruess, and C. I. Steefel (2004), Role of competitive cation exchange on chromatographic displacement of cesium in the vadose zone beneath the Hanford S/SX tank farm, *Vadose Zone J.*, *3*(1), 203–219.

Lu, X., L. Zhang, Y. Wang, J. Shi, and G. Maurer (1996), Prediction of activity coefficients of electrolytes in aqueous solutions at high temperatures, *Ind. Eng. Chem. Res.*, *35*(5), 1777–1784.

Moller, N. (1988), The prediction of mineral solubilities in natural waters: A chemical equilibrium model for the Na-Ca-Cl-SO_4-H_2O system to high temperature and concentration, *Geochim. Cosmochim. Acta*, *52*(4), 821–837.

Monnin, C. (1989), An ion-interaction model for the volumetric properties of natural waters: Density of the solution and partial molal volumes of electrolytes to high concentrations at 25°C, *Geochim. Cosmochim. Acta*, *53*(6), 1177–1188.

Monnin, C. (1994), Density calculation and concentration scale conversions for natural waters, *Comput. Geosci.*, *20*(10), 1435–1445.

Oldenburg, C. M., and K. Pruess (1995), Dispersive transport dynamics in a strongly coupled groundwater-brine flow system, *Water Resour. Res.*, *31*(2), 289–302.

Pabalan, R. T., and K. S. Pitzer (1989), Thermodynamics of concentrated electrolyte mixtures and the prediction of mineral solubilities to high temperatures for mixtures in the system Na-K-Mg-Cl-SO_4-OH-H_2O, *Geochim. Cosmochim. Acta*, *51*(9), 2429–2443.

Park, H., and P. Englezos (1999), Thermodynamic modeling of sodium aluminosilicate formation in aqueous alkaline solutions, *Ind. Eng. Chem. Res.*, *38*(12), 4959–4965.

Pitzer, K. S. (1973), Thermodynamics of electrolytes, I. Theoretical basis and general equations, *J. Phys. Chem.*, *77*, 268–277.

Pitzer, K. S. (1991), Ion interaction approach: Theory and data correlation, in *Activity Coefficients in Electrolytes Solutions*, edited by K. S. Pitzer, pp. 75–155, 2nd ed., CRC Press, Boca Raton, Fla.

Pitzer, K. S., and J. J. Kim (1974), Thermodynamics of electrolytes, IV. Activity and osmotic coefficients for mixed electrolytes, *J. Am. Chem. Soc.*, *96*, 5701–5707.

Pitzer, K. S., and G. Mayorga (1973), Thermodynamics of electrolytes. II. Activity and osmotic coefficients for strong electrolytes with one or both ions univalent, *J. Phys. Chem.*, *77*, 2300–2307.

Plummer, L. N., D. L. Parkhurst, G. W. Fleming, and S. A. Dunkle (1988), A computer program incorporating Pitzer's equations for calculation of geochemical reactions in brines, *U.S. Geol. Surv. Water Resour. Invest. Rep., 88-4153*, 310 pp.

Rimstidt, J. D. (1997), Quartz solubility at low temperatures, *Geochim. Cosmochim. Acta*, *61*(13), 2553–2558.

Rimstidt, J. D., and H. L. Barnes (1980), The kinetics of silica-water interaction, *Geochim. Cosmochim. Acta*, *44*(11), 1683–1699.

Risacher, F., and A. Clement (2001), A computer program for simulation of evaporation of natural waters to high concentration, *Comput. Geosci.*, *27*(2), 191–201.

Samper, J., R. Juncosa, J. Delgado, and L. Montenegro (2000), $CORE^{2D}$: A code for non-isothermal water flow and reactive solute transport, users manual version 2, *Tech. Publ. M-32729-2000*, 131 pp., Empresa Nac. de Residuos Radiactiv., S.A., Madrid.

Silvester, L. F., and K. S. Pitzer (1978), Thermodynamics of electrolytes, 10. Enthalpy and the effect of temperature on the activity coefficients, *J. Solution Chem.*, *7*, 327–337.

Simunek, J., and L. Suarez (1994), Two-dimensional transport model for variably saturated porous media with major ion chemistry, *Water Resour. Res.*, *30*(4), 1115–1131.

Steefel, C. I., S. Carroll, P. Zhao, and S. Roberts (2003), Cesium migration in Hanford sediment: A multisite cation exchange model based on laboratory transport experiment, *J. Contam. Hydrol.*, *67*(1–4), 219–246.

Sun, Y., J. N. Petersen, T. P. Clement, and R. S. Skeen (1999), Development of analytical solutions for multi-species transport with serial and parallel reactions, *Water Resour. Res.*, *35*, 185–190.

van Gaans, P. F. M., and R. D. Schuiling (1997), The waste sulfuric acid lake of the TiO2-plant at Armyansk, Crimea, Ukraine, II. Modeling the chemical evolution with PHRQPITZ, *Appl. Geochem.*, *12*(2), 187–201.

Voss, C. I., and W. R. Souza (1987), Variable density flow and solute transport simulation of regional aquifers containing a narrow freshwater-saltwater transition zone, *Water Resour. Res.*, *23*, 1851–1866.

Wan, J., J. T. Larsen, T. K. Tokunaga, and Z. Zheng (2004a), pH neutralization and zonation in alkaline-saline tank waste plumes, *Environ. Sci. Technol.*, *38*(5), 1321–1329.

Wan, J., T. K. Tokunaga, J. T. Larsen, and R. J. Serne (2004b), Geochemical evolution of highly alkaline and saline tank waste plumes during seepage through vadose zone sediments, *Geochim. Cosmochim. Acta*, *68*(3), 491–502.

Weber, C. F. (2000), Calculation of Pitzer parameters at high-ionic-strengths, *Ind. Eng. Chem. Res.*, *39*(11), 4422–4426.

Weber, C. F., E. C. Beahm, and J. S. Watson (1999), Modeling thermodynamics and phase equilibria for aqueous solutions of trisodium phosphate, *J. Solution Chem.*, *28*(11), 1207–1237.

Wolery, T. J., and S. A. Daveler (1992), EQ6, A computer program for reaction path modeling of aqueous geochemical system: Theoretical manual, user's guide, and related documentation (version 7.0), *UCRL-MA-110662 PT IV*, Lawrence Livermore Natl. Lab., Livermore, Calif.

Xu, T., J. Samper, C. Ayora, M. Manzano, and E. Custodio (1999), Modeling of non-isothermal multi-component reactive transport in field scale porous media flow system, *J. Hydrol.*, *214*(1–4), 144–164.

Yeh, G. T., and V. S. Tripathi (1991), A model for simulating transport of reactive multispecies components: Model development and demonstration, *Water Resour. Res.*, *27*, 3075–3094.

Zhang, G. (2001), Nonisothermal hydrobiogeochemical models in porous media, Ph.D. dissertation, 368 pp., Univ. of La Coruña, La Coruña, Spain.

J. Wan, G. Zhang, and Z. Zheng, Earth Science Division, Lawrence Berkeley National Laboratory, University of California, Berkeley, CA 94720, USA. (gxzhang@lbl.gov)